Biophys Rev (2016) 8:139–149
DOI 10.1007/s12551-016-0196-8

REVIEW

Protein–DNA and ion–DNA interactions revealed through contrast variation SAXS

Joshua M. Tokuda[1] · **Suzette A. Pabit**[1] · **Lois Pollack**[1]

Received: 28 January 2016 / Accepted: 10 March 2016 / Published online: 2 April 2016

Abstract Understanding how DNA carries out its biological roles requires knowledge of its interactions with biological partners. Since DNA is a polyanionic polymer, electrostatic interactions contribute significantly. These interactions are mediated by positively charged protein residues or charge compensating cations. Direct detection of these partners and/or their effect on DNA conformation poses challenges, especially for monitoring conformational dynamics in real time. Small-angle x-ray scattering (SAXS) is uniquely sensitive to both the conformation and local environment (i.e. protein partner and associated ions) of the DNA. The primary challenge of studying multi-component systems with SAXS lies in resolving how each component contributes to the measured scattering. Here, we review two contrast variation (CV) strategies that enable targeted studies of the structures of DNA or its associated partners. First, solution contrast variation enables measurement of DNA conformation within a protein–DNA complex by masking out the protein contribution to the scattering profile. We review a specific example, in which the real-time unwrapping of DNA from a nucleosome core particle is measured during salt-induced disassembly. The second method, heavy atom isomorphous replacement, reports the spatial distribution of the cation cloud around duplex DNA by exploiting changes in the scattering strength of cations with varying atomic numbers. We demonstrate the application of this approach to provide the spatial distribution of monovalent cations (Na^+, K^+, Rb^+, Cs^+) around a standard 25-base pair DNA. The CV strategies presented here are valuable tools for understanding DNA interactions with its biological partners.

Keywords SAXS · Contrast variation · NCP · DNA · Ions · Heavy atom isomorphous replacement

✉ Lois Pollack
lp26@cornell.edu

[1] School of Applied and Engineering Physics, Cornell University, Ithaca, NY 14853, USA

Introduction

The double helical structure of DNA enables the efficient storage, replication, repair and transcription of this fundamental macromolecule. These functions and others require macromolecular partners, and are carried out on the background of physiological solutions with ionic strengths that exceed 0.1 M (Mouat and Manchester 1998). Because of the high negative charge of the DNA backbone, long-range electrostatic forces affect DNA's interactions with essential cellular partners. These partners range in size and complexity from small cations to large macromolecular protein complexes (Bloomfield et al. 2001; Martin and Saenger 2013).

The majority of macromolecules that interact with DNA are proteins (Luscombe et al. 2000; Hernan et al. 2007; Luger and Phillips 2010; Rohs et al. 2010). Many DNA binding proteins possess positively charged side chains and exploit electrostatics in their interactions with DNA's backbone (Korolev et al. 2007). For example, positively charged regions in histone proteins help fold DNA into stable structures that lead to efficient storage in chromatin (Clark and Kimura 1990; Widom 1998; Hansen 2002; Korolev et al. 2010; Andrews and Luger 2011). Not all interactions are passive, as enzymes like helicases exploit electrostatic interactions to actively unwind DNA (Thommes and Hubscher 1992; Liu et al. 2009).

In addition to proteins, smaller, charged molecules also serve as essential partners of DNA (Wong and Pollack 2010). They are more challenging to study because, unlike

many DNA-binding proteins, these smaller molecules or ions can interact non-specifically with DNA structures and are therefore not amenable to characterization by standard methods like x-ray crystallography. Because much of the charge compensation of DNA in cells is accomplished by small salt ions, a detailed understanding of their interactions with DNA is essential in gaining an accurate view of electrostatic interactions between DNA and other partners, including proteins (Lohman and Overman 1985). Simple systems such as DNA duplexes in salt solutions of monovalent or divalent ions are important benchmarks for modeling electrostatic effects and are essential for validating force fields or theories that accurately capture DNA electrostatics (Anderson 1995; Zuo et al. 2006; Park et al. 2009; Nguyen et al. 2014; Meisburger et al. 2015). Accurate and experimentally validated parameters are essential for developing models of protein–DNA interactions.

Our understanding of DNA is intricately linked with knowledge of how it interacts with partners. In this review, we describe recent updates to two contrast variation (CV) methods employed with solution small-angle x-ray scattering (SAXS) that highlight the interactions between DNA and protein or solvent/ion partners. The first example describes the use of dense solvents to mask the scattering of proteins in a protein–DNA system. In conjunction with time-resolved methods and changing solution conditions, contrast variation SAXS provides new insights into the electrostatic interactions that stabilize protein–DNA complexes, as well as DNA conformational changes within these complexes. We also discuss recent progress in using heavy atom replacement methods to quantify the hydration and ionic environment around double-stranded DNA. The new information provides stringent tests of theories and also yields fundamentally important information about the ubiquitous, but difficult to visualize partners that influence DNA interactions with all other molecules in the cell.

General SAXS overview and two contrast variation strategies

We begin with a brief overview of solution SAXS, a remarkably simple, yet powerful technique that provides information about the structures of biological macromolecules. SAXS studies can be easily carried out under a variety of solution conditions and as a function of time, allowing ready access to measurements of large-scale conformational changes and assembly/disassembly processes important for biological function (Lipfert and Doniach 2007; Jacques and Trewhella 2010; Skou et al. 2014). Recent advances in x-ray sources, data collection and analysis tools have greatly expanded the biological problems that may be investigated with SAXS (Pérez and Nishino 2012; Graewert and Svergun 2013; Vestergaard and Sayers 2014; Chaudhuri 2015; Curry 2015). The theoretical principles behind SAXS and novel applications are covered in great detail in other reviews (Koch et al. 2003; Svergun and Koch 2003). Here, we provide only the relevant introductory information to understand the contrast variation methods, whose application to DNA–partner interactions is the subject of this review.

The SAXS signal originates as illustrated in Fig. 1, when a dilute solution of macromolecules is exposed to x-rays. X-rays scatter elastically in response to electron density variations throughout the illuminated volume, and yield a diffraction pattern. Although the spatial and orientational averaging of macromolecules in solution result in a loss of atomic-scale resolution, the resulting 1-dimensional intensity profile contains information about macromolecular features with a resolution that is typically of order 10 Å for SAXS. Global structural properties such as molecular weight, radius of gyration, and low-resolution shape envelopes are readily obtained for any homogeneous macromolecular system. However, in the case of multi-component systems (e.g., protein–DNA complexes, or DNA and its ion cloud), interpretation of SAXS data is obscured by our limited ability to discern how each component contributes to the total scattering.

In order to understand the principles behind these contrast variation approaches, we briefly discuss the origin of the SAXS signal (for more details, see Guinier and Fournet 1955; Glatter and Kratky 1982). In most SAXS experiments, macromolecules have a higher electron density than the solvent that surrounds them. This density difference gives rise to the scattering, and can be expressed in terms of the (average) electron density difference between the macromolecule and the solution: $\Delta\rho_M = \rho_M - \rho_{solv}$. The number of excess electrons present in the volume occupied by the macromolecule (relative to an identical volume occupied by the solvent) is given by the scattering factor: $f_1 = \Delta\rho_M\ V_M$, where V_M indicates the volume of the macromolecule. If the macromolecule were in vacuum, f_1 would equal the number of electrons present in the macromolecule. Since the solvent is essential for physiological measurements, the relevant value reflects the number of *excess* electrons above that contained by the solvent in the same volume.

The amplitude of the SAXS signal is described by the product of this scattering factor, f_1, and an angle (or q)-dependent form factor, $F_1(q)$, that reflects the arrangement of electrons in the macromolecule. For a single component system, the scattering amplitude is given by: $A = f_1\ F_1(q)$. This equation neglects density fluctuations internal to the macromolecule (Svergun and Koch 2003). SAXS experiments measure intensity: the product of the scattering amplitude and its complex conjugate. For a single particle system, this "squaring" is

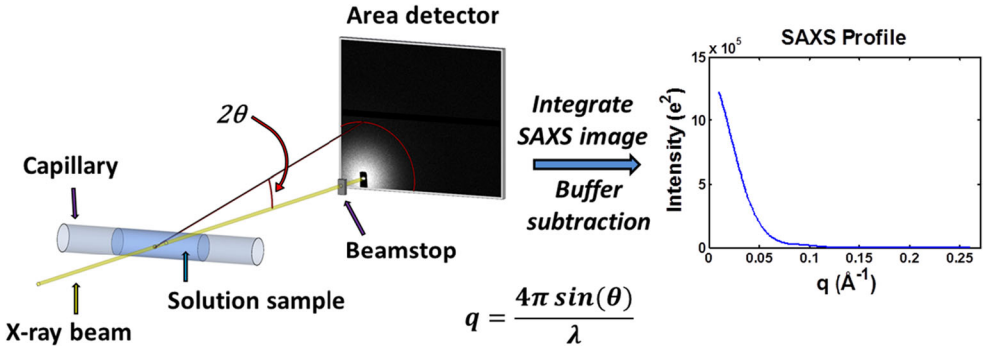

Fig. 1 Small-angle X-ray scattering (SAXS) is a solution-based approach that yields the low-resolution structures of macromolecules. *Left* A schematic of a typical SAXS experiment is shown. The sample is typically a buffered solution containing 2 mg/mL of protein, DNA, or protein–DNA complex. This sample oscillates through a quartz capillary to reduce radiation damage from the x-ray beam. The scattered x-rays are imaged onto an area detector while the primary beam is either blocked or greatly attenuated (as shown) by a beamstop. *Right* The images are pooled, averaged, and converted into profiles of intensity as a function of scattering vector, $I(q)$, through azimuthal integration. For each sample, a corresponding measurement of the buffer alone is made and the resulting buffer profile is subtracted from the sample profile to obtain the macromolecular SAXS profile. SAXS intensities can be calibrated onto an absolute scale (in units of e^2) through the measurement of water as a standard

not of concern. The measured scattering intensity can be written as:

$$I(q) = f_1{}^2\, P_1(q), \tag{1}$$

where $P_1(q)$ is the partial scattering form factor of this molecule, given by $F_1(q)F_1{}^*(q)$ integrated over all space. $P_1(q)$ reflects the shape of the macromolecule and is unity at $q=0$.

For a two-component system, the total scattering amplitude is the sum of that from each component: $A=f_1F_1(q)+f_2F_2(q)$, where the subscripts reflect each of the two components. The resulting expression for scattering intensity contains cross terms, proportional to various products of the form factors, $F_1(q)$ and $F_2(q)$. These terms, which depend on the structures of both particles, introduce new challenges and present new opportunities for the study of multicomponent systems (i.e. DNA–protein, or DNA–ion). For this system, the scattering intensity $I(q)$ is given by:

$$I(q) = f_1{}^2\, P_1(q) + 2f_1f_2P_{12}(q) + f_2{}^2P_2(q), \tag{2}$$

where $P_1(q)$ and $P_2(q)$ are the partial scattering form factors for each of the two components and reflects their individual contributions. The cross term, $P_{12}(q)$, contains information about the relative distributions of electrons between the two components.

The two experimental strategies we describe vary the scattering factors (f_1 or f_2) in the above equations. In solution contrast variation, which is applied to DNA–protein systems, the solvent is manipulated to eliminate the contribution from one of the components. If DNA is component 1 and a protein partner is component 2, the contrast variation experiment essentially drives f_2 to zero. In the second method, heavy atom isomorphous replacement, consider the case where DNA is component 1 and the ion cloud is component 2. Varying f_2 in a predictable way leads to a solvable system of simultaneous equations, which allows us to extract both the cross term and the much weaker scattering term P_2, providing the distribution of counterions. Absolute calibration of the intensities allows us to extrapolate to the case of $f_2=0$, providing information about the hydrating waters associated to the DNA.

Principles behind solution contrast variation

Solution contrast variation (Fig. 2) allows the SAXS signal from individual components to be measured within a multicomponent complex if the components have different electron densities. The signal is isolated by varying the electron density of the bulk solvent until it matches that of one of the components. Under this condition, the matched component no longer contributes to the measured signal and details from the remaining components can be obtained. This approach is detailed in Stuhrmann and Kirste (1965), Jacques and Trewhella (2010), and Svergun et al. (2013). Below, we demonstrate how solution CV can be applied to reveal the conformational details of DNA within a protein–DNA complex. This information is valuable when addressing important issues, for example, understanding how proteins modulate DNA structure for further processing in the cell.

If component 1 represents the DNA and component 2 represents the protein, then Eq. 2 can be rewritten as:

$$I(q) = f_{DNA}{}^2\, P_{DNA}(q) + 2f_{DNA}f_{prot}P_{DNA\cdot prot}(q) + f_{prot}{}^2P_{prot}(q), \tag{3}$$

where f_{DNA}, $P_{DNA}(q)$ and f_{prot}, $P_{prot}(q)$ represent the scattering factors and partial form factors for the two components, respectively. $P_{DNA\cdot prot}(q)$ is the cross-term form factor. The

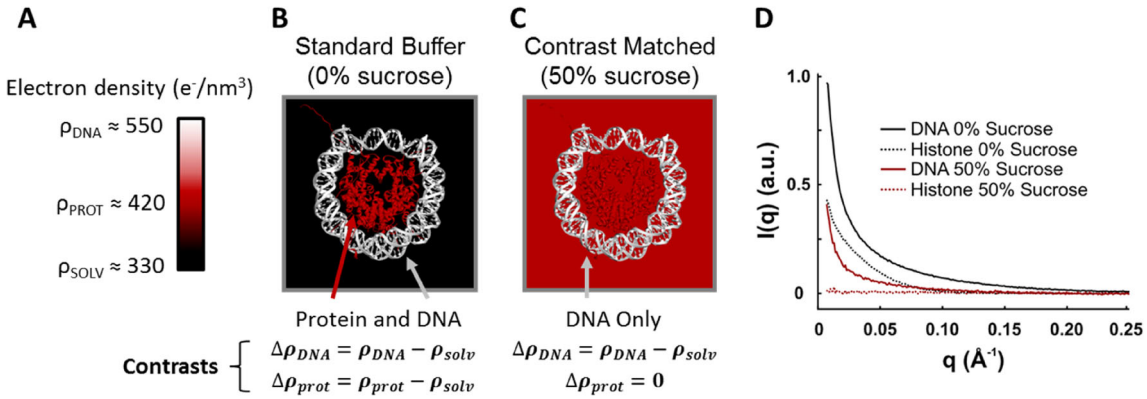

Fig. 2 Cartoon illustration of the principle behind solution contrast variation. **a** A color scale bar is shown with average electron density values for DNA, protein, and water. **b**, **c** Cartoon schematics of the nucleosome core particle (1AOI, Luger et al. 1997) in buffers with electron densities that vary according to the addition of 0 % (**b**) and 50 % (**c**) sucrose. The resulting contrasts (excess electron densities) are shown below each condition. **d** SAXS profiles for the DNA and histone proteins measured separately with and without sucrose. Note: in 50 % sucrose, the histone SAXS signal disappears, but the DNA is still visible due to its higher electron density

scattering factors are related to electron densities as $f_{DNA} \propto (\rho_{DNA} - \rho_{solv})$ and $f_{prot} \propto (\rho_{prot} - \rho_{solv})$. If the solvent electron density (ρ_{solv}) is increased to equal that of the protein (ρ_{prot}), then $f_{prot} = 0$ and the second and third terms of Eq. 3 vanish (note: Eq. 3 becomes Eq. 1, which describes a single component system). As stated above, this analysis does not account for internal density fluctuations within the DNA or protein components—a valid approximation in most cases since these fluctuations are typically much smaller that the differences between the components. Nevertheless, the resulting scattering profile is dominated by the DNA shape and conformational details of the DNA emerge that are otherwise obscured in standard SAXS measurements. The addition of 50–65 % (w/v) sucrose to the solvent typically suffices to match the electron density of most proteins. Note that the effective scattering factor for the DNA is also reduced when the solvent electron density is increased, which results in a weaker but otherwise unchanged signal. This approach is visualized in Fig. 2.

Theoretically, if the electron density of the solvent was increased further to match that of the DNA, the protein signal from the complex can be isolated. Sucrose cannot be used to achieve this matching condition due to solubility limits; however, the use of other highly soluble additives with heavier atoms may enable such studies in the future. Small-angle neutron scattering (SANS) is better suited for this type of contrast matching due to the remarkable difference in scattering between hydrogen and deuterium. In SANS, the scattering from various components can be selected by varying the H_2O/D_2O composition of the solvent. This approach has been applied with great success in the pioneering studies of nucleosomes (Baldwin et al. 1975; Bram et al. 1975; Pardon et al. 1975) as well as a variety of other biomolecular complexes (Stuhrmann and Kirste 1965; Hjelm et al. 1977; Svergun et al. 1994, 2013; Svergun and Koch 1994; Jacques and Trewhella 2010). Solution CV has proven to be a powerful tool in SAXS studies for elucidating the structural details of multi-component systems in which each component has a distinct electron density. Measurements carried out at multiple contrast levels can be used to identify the best match point for one component, or to reveal finer structural details. Though outside the scope of work described here, these approaches have been described (Ibel and Stuhrmann 1975; Sardet et al. 1976; Tardieu et al. 1976; Ueki et al. 1986; Inoko et al. 1992). Recent advancements in x-ray technologies and high flux of x-ray sources significantly decreases the measurement time and uniquely enables time-resolved studies (Chen et al. 2014). Contrast variation SAXS and SANS methods have been reviewed (Stuhrmann 1974; Stuhrmann and Miller 1978; Jacques and Trewhella 2010; Svergun et al. 2013).

Solvent CV SAXS reveals partially unwrapped states for DNA in nucleosome core particles

The power of solvent CV methods to reveal biologically important changes in a protein–DNA system is highlighted in recent studies that focus on the salt-induced disassembly of nucleosomes (Chen et al. 2014). To package and regulate access to nuclear genetic information, eukaryotic cells organize the DNA in repeated structural units called nucleosome core particles (NCPs) (Kornberg and Lorch 1999; Andrews and Luger 2011). NCPs consist of approximately 147 base pairs (bp) of DNA wrapped in ≈1.7 superhelical turns around a symmetric octamer of histone proteins. Although high-resolution structures for the most stable conformations have been well characterized (Luger et al. 1997; Richmond and Davey 2003), little is known about the transient and partially unwrapped structures relevant to nucleosome dynamics (Li and Widom 2004; Mihardja et al. 2006; Gansen et al. 2009a, b; Shlyakhtenko et al. 2009; Zlatanova et al. 2009; Prinsen and Schiessel 2010; Tims et al. 2011; Li and Wang 2012; Ngo

et al. 2015; Ngo and Ha 2015; Vlijm et al. 2015). These dynamics regulate the accessibility of DNA for processing by proteins. Since these protein–DNA interactions are mediated by electrostatic interactions, the addition of salt weakens the protein's affinity for the DNA, and populates partially disrupted species (Yager et al. 1989; Hoch et al. 2007; Gansen et al. 2009a, 2015; Buning and Van Noort 2010). Contrast variation is an ideal method to monitor DNA release as the complex is destabilized by salt.

The first step in a solvent CV experiment is to determine how much sucrose needs to be added to increase the density of the buffer until it matches that of the proteins (Fig. 2c). To accomplish this goal, SAXS profiles of isolated histone proteins are acquired in solutions containing different concentrations of sucrose. In 50 % (w/v) sucrose, the protein signal was effectively eliminated (Fig. 2d). Because variations in the sucrose concentration can lead to small changes in scattering, one of the greatest challenges associated with this technique is the need to closely match the sucrose concentration in the buffer sample with that of the NCP sample. SAXS profiles of the DNA alone were also acquired at this solution condition, and confirmed that sufficient signal exists to determine DNA conformation. In this case, where it is possible to extract only the scattering of one component in a multicomponent system, it is straightforward to compute the pairwise distance distribution function, P(R), which is related to the Fourier transform (FT) of the SAXS profile as shown in Eq. 4 (Svergun and Koch 2003):

$$P(R) = \frac{1}{2\pi^2}\int_0^\infty I(q)\cdot qR\cdot \sin(qR)dq. \quad (4)$$

In practice, only approximate solutions for P(R) are obtained through indirect Fourier transform methods due to experimental limitations (e.g., finite measureable q-range). Detailed instructions for obtaining reliable P(R) curves are reviewed in Skou et al. (2014). This procedure allows a conversion of SAXS data from reciprocal (q) to real space (R), and can be very informative if well-defined shapes are present. Peaks in the P(R) distributions represent length scales that are prominent or repeated in the particles, and assist in interpreting structural changes reported by SAXS. These P(R) computations are relatively straightforward to apply using readily available software such as GNOM (Svergun 1992).

SAXS profiles were measured (q-range: 0.007–0.26 $Å^{-1}$) for NCPs equilibrated in buffers with NaCl concentrations ranging from 0.2 to 2.0 M. At low salt concentrations, the DNA is stably wound around the histone core. At high salt concentrations (≈ 2 M NaCl), complete dissociation is observed, and the DNA assumes a rod-like shape due to its long persistence length (Hagerman 1988; Marko and Siggia 1995; You et al. 2012). These expected end states (fully wrapped vs. fully released) are shown in Fig. 3a. Figure 3b shows pairwise distance distributions, P(R), computed from data acquired on NCP particles in a salt titration without sucrose. In 0.2 M NaCl, the NCPs are compact with the DNA predominantly wrapped tightly. The general extension observed in the P(R) curves as the salt concentration increases reflects the increasing population of partially unwrapped species. However, the trends observed in the P(R) curves are extremely challenging to interpret when both protein and DNA scatter. The addition of sucrose to mask the signal from the protein significantly clarifies the situation and illustrates the power of this approach.

When the NCP in the same salt series is measured with 50 % sucrose, the protein scattering is effectively eliminated and identifiable features emerge from the P(R) distributions

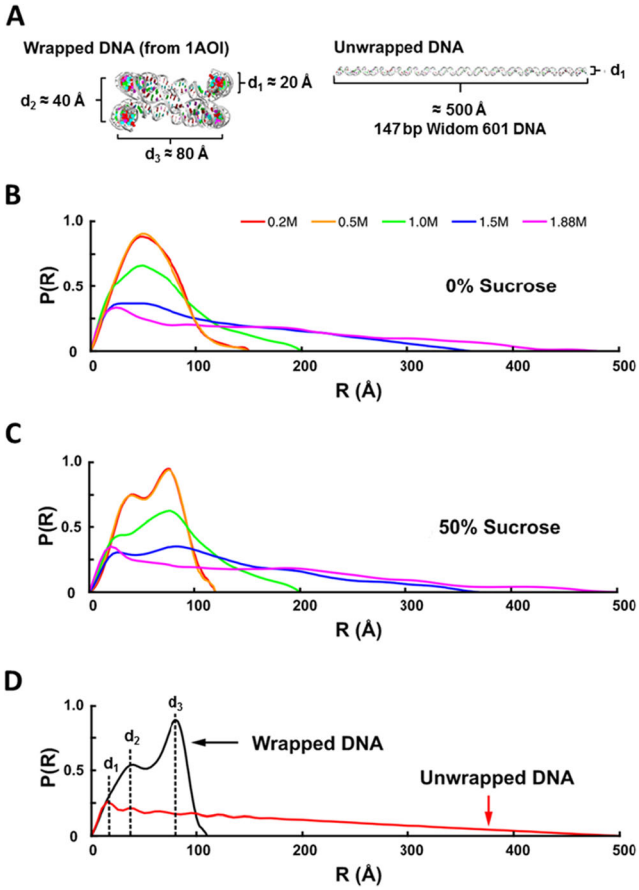

Fig. 3 Application of solution contrast variation to monitor DNA unwrapping during the salt-induced disassembly of nucleosome core particles (NCP). **a** DNA models for the expected end states of the NCP at low [NaCl] (completely wrapped) and high [NaCl] (completely unwrapped). **b** P(R) curves for the NCP measured in 0 % sucrose and varied [NaCl]. **c** P(R) curves for the NCP measured in 50 % sucrose and varied [NaCl]. **d** P(R) curves determined for the models in (**a**). Peaks in the P(R) curves can be associated with structural features as follows: d_1, diameter of the duplex DNA; d_2, distance between overlapping DNA ends; d_3, diameter of the overall wrapped structure. These curves, specifically the difference between P(R) illustrate highlight how structural features emerge in the contrast matched condition

(Fig. 3c). These peaks reveal conformational details of the nucleosomal DNA with varying degrees of unwrapping. In order to interpret these features, the peaks are compared with theoretical P(R)s (Fig. 3c) calculated for the expected end states of Fig. 3a. As the DNA unwraps with increasing salt, several trends proceed as follows: (1) the peak at $d_1 \approx 20$ Å increases, reflecting the extension of duplex DNA, (2) the peak at $d_2 \approx 40$ Å decreases, coinciding with the reduction of overlap between the DNA ends, and (3) the peak at $d_3 \approx 80$ Å decreases, corresponding to the disruption of the overall wrapped structure. These results illustrate the advantage of applying solution contrast variation to provide insight into DNA conformation within a protein–DNA complex.

In order to visualize the DNA conformations present at each salt concentration, the SAXS profiles collected for NCPs in 50 % sucrose can be used as a constraint to select DNA conformations that best recapitulate the data. This approach is preferred over ab initio reconstructions which struggle to generate certain structural features (e.g., holes, as found in wrapped DNA, and structures with large aspect ratios, as found in unwrapped DNA). First, a pool of DNA structures is generated with varying degrees of unwrapping (see methods in Chen et al. 2014). Since multiple DNA conformations may be present at each salt concentration, a genetic algorithm selects an ensemble of structures that produce SAXS profiles that best match the data at each condition. Although this approach, called ensemble optimization method (EOM) (Bernadó et al. 2007; Bernadó and Svergun 2012), was initially designed for flexible proteins, this strategy has been successfully adapted to identify conformational details of nucleic acids measured with SAXS (Stoddard et al. 2010; Kazantsev et al. 2011; Gopal et al. 2012; Chen et al. 2014). An example fit of the experimental data with the theoretical profile generated from the ensemble selected for the data collected at 1.0 M NaCl and 50 % sucrose is shown in Fig. 4a. The DNA models selected for each salt concentration are shown in Fig. 4b. These structures independently confirm the interpretation of the P(R) curves provided above, and highlight the power of this approach for determining the structures of DNA within protein–DNA complexes.

The combination of this approach with time-resolved methods available at bright x-ray synchrotron sources uniquely enables measurements of the dynamics of the conformational change. Chen et al. proceeded to resolve transient structures with millisecond time resolution by incorporating a stopped flow mixer that effected a salt jump from the initial, wrapped state (0.2 M) to the final extended state (≈ 2 M). A transient, asymmetric state was detected, with a short lifetime of about 1 s. This DNA conformation may serve as an important biological substrate for gene regulation.

CV-SAXS methods that focus on DNA's partners: water and counterions

In the absence of protein partners, DNA is surrounded by charge compensating salt ions and water (Manning 1969; Draper 2004). A full understanding of biological processes requires knowledge of the solvent structure around DNA as binding and release of these small ions and molecules facilitate all other interactions (Lohman and Overman 1985; Wong and Pollack 2010; Lipfert et al. 2014). Commonly applied electrostatic theories that describe the structure and composition of salt ions in the solvent are based on mean-field treatments, for example the Poisson–Boltzmann equation (Chin et al. 1999; Grochowski and Trylska 2007). Although these theoretical treatments are straightforward to apply, they insufficiently capture the details necessary to fully describe ion–DNA interactions (Bardhan 2012). Improved theories with varying degrees of sophistication have been proposed to predict the spatial arrangement of ions around DNA (Holst et al. 2000; Rocchia et al. 2001; Das et al. 2003; Tang et al. 2004; Bai et al. 2007; Chu et al. 2007; Giambaşu et al. 2014; Nguyen et al. 2014). However, assessment of the validity of any approach requires comparison with measurements that are sensitive to DNA's ionic and solution environment. Contrast

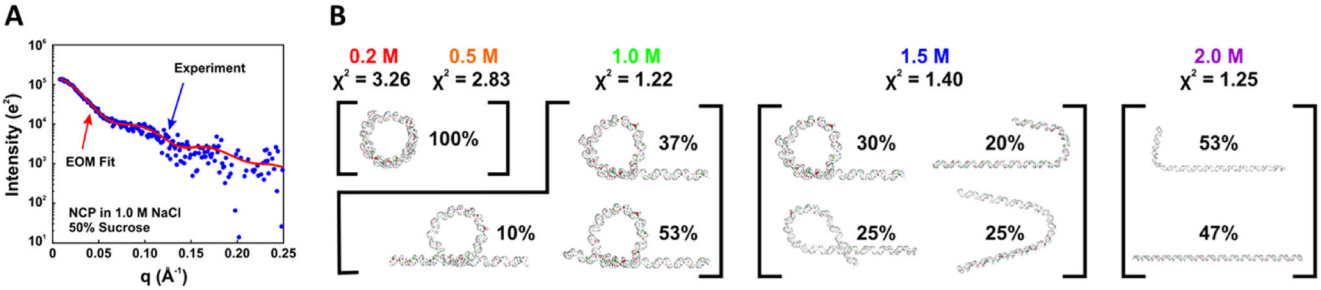

Fig. 4 DNA models selected by ensemble optimization method (*EOM*) that best recapitulate the [NaCl]-dependent SAXS data for NCPs measured in 50 % sucrose. **a** Fit of the experimental data collected at 1.0 M NaCl with the theoretical SAXS curve generated from the ensemble of structures selected by EOM. Similar fits (not shown) were found for other [NaCl] concentrations. **b** Models representing the ensemble of structures selected by EOM that generate SAXS profiles that best fit the data measured at the indicated salt concentrations. χ^2 values assessing the overall fit to the experimental data and percentages reporting the weight of each model are shown. These models show how the DNA unwraps with increasing [NaCl]

variation SAXS methods offer several ways to detect localized but not exclusively site bound ions.

Anomalous SAXS, or ASAXS, has been successfully used to count the number of excess positively charged counterions around nucleic acids relative to the number that would exist in solution without the DNA (Pabit et al. 2009b, 2010). ASAXS also provides their positions relative to the macromolecule (Andresen et al. 2004, 2008; Ballauff and Jusufi 2006; Pabit et al. 2009a; Pollack 2011; Sztucki et al. 2012). Here, the counterion contrast is varied by probing the system with different energy x-rays. If the x-ray energy is close to the binding energy of a core electron in a particular element, its scattering strength is reduced relative to a measurement far from this atomic absorption edge (Bradley et al. 2006a, b). Measurements at different energies can be used to vary the contrast of one atomic species within a sample. These energy-dependent changes can be exploited to provide the information of interest. ASAXS methods have been recently reviewed in Pabit et al. (2009a), and will not be discussed here. Instead, we revisit the method of heavy atom isomorphous replacement, as previously used to study ions around DNA (Luzzati 1967; Chang et al. 1990; Das et al. 2003; Morfin et al. 2004; Meisburger et al. 2015). Recently, this method was powerfully updated (Meisburger et al. 2015) by combining absolute calibration with a new systematic approach that solves a series of simultaneous equations, carried out at different values of counterion contrast.

Heavy atom isomorphous replacement reveals the number and spatial distribution of monovalent ions around DNA

In heavy atom isomorphous replacement, the strength of the scattering from the ion atmosphere is systematically varied by substituting the associated ions with heavier counterparts. Recent work focused on measurements of a series of monovalent ions around dilute, non-interacting solutions of 25-bp DNA ([DNA] = 50 μM). The duplex was buffer-exchanged extensively in different salt solutions, containing either 100 mM NaCl, KCl, RbCl, or CsCl and 1 mM Na-MOPS, pH 7.0. Returning to Eq. 2, if the DNA is component 1 and the ions are component 2, the scattering intensity from these ion–DNA systems is represented as follows:

$$I(q) = f_M{}^2 P_M(q) + 2f_M(N_{Ion}f_{Ion})P_{MI}(q) + (N_{Ion}f_{Ion})^2 P_I(q), \quad (5)$$

where f_M is the number of excess electrons contributed by the DNA and its associated water molecules, N_{Ion} and f_{Ion} are the number of associated counterions and the number of excess electrons per ion, and $P_M(q)$ and $P_I(q)$ are the partial scattering factors associated with the hydrated macromolecule and the counterions. $P_{MI}(q)$ is the cross term, with contributions from both the structure of the macromolecule and the ions.

The use of different counterions (with known values of contrast) is equivalent to varying f_{Ion} and yields a series of simultaneous equations that can be solved to extract information about DNA hydration and the distribution of counterions. This strategy is illustrated in Fig. 5a, where progressively larger ions are distributed around a DNA duplex. An underlying assumption for this analysis is that the ion distribution remains the same, despite the increase in atomic number.

These experiments benefit from absolute calibration of the data (Orthaber et al. 2000). Here, the measured intensity on the detector is converted into absolute scattering strength in terms of the square of the number of electrons in the sample. Equation 5 reveals a very useful application of this calibration. At $q = 0$, the form factors are unity: $P_M(0) = P_{MI}(0) = P_I(0) = 1$. Therefore, we can write:

$$I(q = 0) = (f_M + N_{Ion}f_{Ion})^2. \quad (6)$$

Here, f_{Ion} is the effective number of electrons, derived from the number of electrons per ion (in vacuum) minus the density of the solvent times the partial molar volume of the ion (Meisburger et al. 2015). Figure 5b shows the scattering profiles of DNA in the presence of the different monovalent ions. Note the increased scattering signal as the compensating cations increase in atomic number. A fit to the data provides the value of $I(q = 0)$, which can be used in the above equation.

Given the linear nature of Eq. 6, a plot of the $\sqrt{I}(0)$ versus f_{Ion} in Fig. 5c yields the value of f_M as the y-intercept. This value of f_M includes information about the number of tightly associated waters as discussed in detail in Meisburger et al. (2015). The slope of the line provides the number of ions, N_{Ion}. For the case of monovalent ions around DNA, the value obtained, 36.5 ± 2.4, is in good agreement with ion counting via ASAXS measurements, 39 ± 2 (Pabit et al. 2010; Nguyen et al. 2014). The straight line validates our assumption of identical distributions for the different monovalent ions. All these parameters provide useful experimental benchmarks for comparison with theories of ion and water association to DNA.

In addition, the partial scattering form factors $P_M(q)$, $P_{MI}(q)$, $P_I(q)$ can be extracted from the data for comparison to theory. Figure 6 shows the partial scattering form factors scaled by the scattering factors determined for Rb (terms from Eq. 5). Most useful are the latter two curves, which reflect the ion–DNA interference term, and the pure ion scattering term. We note that a similar decomposition can be used in ASAXS to extract these terms if measurements at more than three energies are acquired (Ballauff and Jusufi 2006). However, the ion contributions measured using heavy atom isomorphous replacement can be obtained with greater

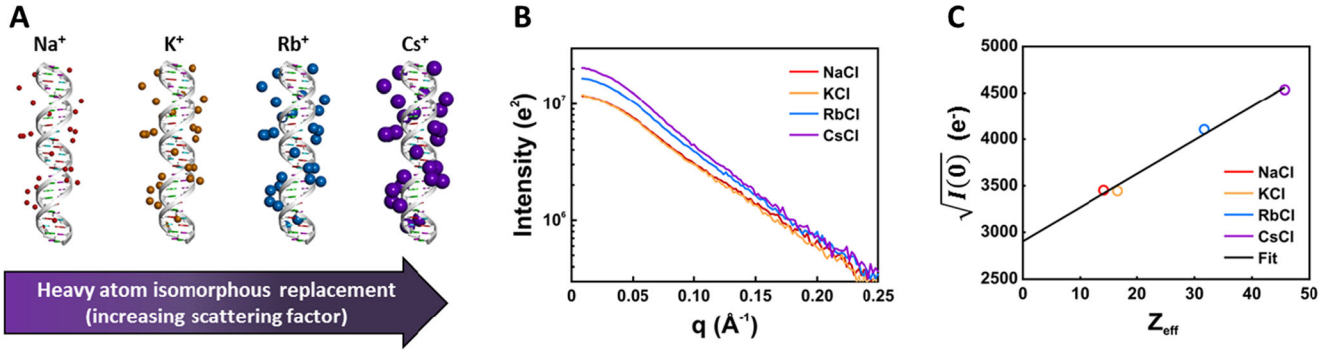

Fig. 5 Application of heavy atom isomorphous replacement to study the ion atmosphere around a 25-base pair DNA duplex. **a** Cartoon illustration of how increasing the atomic number of the monovalent cation cloud affects the scattering profile of the DNA–ion system. Ion size differences have been exaggerated to emphasize the increasing scattering factor. The dynamic spatial distributions of the different species of cations are assumed to be the same. **b** SAXS profiles for 50 μM DNA measured in 100 millimolar solutions of the monovalent chloride salts shown in (**a**). The increasing contrast for the heavier cations results in larger scattering signals. **c** The square root of the extrapolated forward scattering is shown to vary linearly with the effective ion contrast (see Eq. 5). This linearity is consistent with the assumption that the number and arrangement of these (excess) cations are identical (Meisburger et al. 2015)

signal-to-noise relative to ASAXS since the relevant ion scattering signal (third term in Eq. 5) is significantly larger than that measured from the anomalous signal (Pabit et al. 2009a). The shapes of the ion–DNA and ion scattering terms provide insight into the spatial arrangement of ions around the DNA and can be used to assess theoretical models of the ion cloud. As shown in Meisburger et al. (2015), comparison of these shape-functions to predicted scattering profiles based on the non-linear Poisson Boltmann equations suggest that this mean field theory underestimates the number of ions present near the DNA surface.

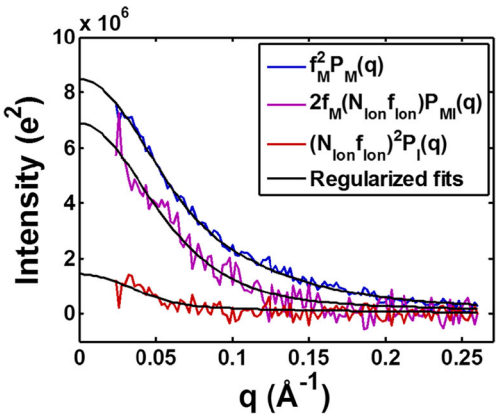

Fig. 6 Mathematical decomposition of the measured scattering of DNA duplexes and associated ions into contributions from partial structure factors. Shown here are the terms in Eq. 4 calculated for the DNA surrounded by a cloud of Rb^+ ions. Details for this calculation are provided in Meisburger et al. (2015). Regularized fits to the data (*black*) were calculated using GNOM (Svergun 1992). Since DNA is always surrounded by a cloud of charge compensating ions, the mathematical decomposition illustrates the strong contributions of the DNA–ion cross term and the ion–ion scattering to the scattering profile of the DNA–ion system

Conclusions and outlook

This review focused on recent developments in measuring the distribution of partner molecules that are critical to the structure and function of DNA, demonstrating how SAXS contrast variation methods can be applied to focus on one component in a multi-component system. The first example illustrated how the contributions from lower density proteins could be 'masked' in a protein–DNA system, to reveal only the scattering from the DNA. The second example illustrated how the scattering from counterions could be enhanced in an ion–DNA system to extract critical information about their number and distribution around DNA. The overall goal of this work is to enable measurements that focus on only one component, although both are present. This strategy allows for more direct comparison with predictions and elucidates DNA interactions with its biological partners.

Although neither contrast variation, nor heavy atom replacement techniques are new, the advent of high brightness x-ray sources enables the new opportunities described here. For the case of the counterion scattering, the large signal sizes (relative to the noise) allows the extraction of weaker terms, such as the ion partial scattering factor. Extension to ions of higher valence is in progress, but caution must be exercised to ensure that the assumption about identical ion distribution holds. For divalent ions, specific interactions are known to occur, which may alter ion distributions according to ion type.

It is also exciting to consider future opportunities to monitor structural dynamics by the inclusion of time-resolved methods with the solvent contrast variations methods described. Time resolution as short as 10 ms has recently been demonstrated (manuscript in preparation), and extension to longer time scales, as warranted by the biological questions, is also possible. This tool can also be extended to the study of RNA–protein systems. Planned experiments include watching

enzymes, such as polymerases or helicases, as they modify nucleic acid substrates in real time, as well as the ejection of genomic material from viruses.

Acknowledgments The work was supported by National Institutes of Health grants (EUREKA R01-GM088645) and (R01-GM085062). J.M.T. was supported by National Institutes of Health Training Grant (T32GM008267).

Compliance with ethical standards

Conflict of interest Joshua M. Tokuda declares that he has no conflict of interest.

Suzette A. Pabit declares that she has no conflict of interest.

Lois Pollack declares that she has no conflict of interest.

Ethical approval This article does not contain any studies with human participants or animals performed by any of the authors.

References

Anderson CF (1995) Salt-nucleic acid interactions. Annu Rev Phys Chem 46:657–700

Andresen K, Das R, Park HY et al (2004) Spatial distribution of competing ions around DNA in solution. Phys Rev Lett 93:248103. doi:10.1103/PhysRevLett.93.248103

Andresen K, Qiu X, Pabit SA et al (2008) Mono- and trivalent ions around DNA: a small-angle scattering study of competition and interactions. Biophys J 95:287–295. doi:10.1529/biophysj.107.123174

Andrews AJ, Luger K (2011) Nucleosome structure(s) and stability: variations on a theme. Annu Rev Biophys 40:99–117. doi:10.1146/annurev-biophys-042910-155329

Bai Y, Greenfeld M, Travers KJ et al (2007) Quantitative and comprehensive decomposition of the ion atmosphere around nucleic acids. J Am Chem Soc 129:14981–14988. doi:10.1021/ja075020g

Baldwin JP, Boseley PG, Bradbury EM, Ibel K (1975) The subunit structure of the eukaryotic chromosome. Nature 256:245–249

Ballauff M, Jusufi A (2006) Anomalous small-angle X-ray scattering: analyzing correlations and fluctuations in polyelectrolytes. Colloid Polym Sci 284:1303–1311. doi:10.1007/s00396-006-1516-5

Bardhan JP (2012) Biomolecular electrostatics—I want your solvation (model). Comput Sci Discovery 5:013001. doi:10.1088/1749-4699/5/1/013001

Bernadó P, Svergun DI (2012) Structural analysis of intrinsically disordered proteins by small-angle x-ray scattering. Mol BioSyst 8:151–167. doi:10.1039/C1MB05275F

Bernadó P, Mylonas E, Petoukhov MV et al (2007) Structural characterization of flexible proteins using small-angle x-ray scattering. J Am Chem Soc 129:5656–5664. doi:10.1021/ja069124n

Bloomfield VA, Crothers DM, Tinoco JI (2001) Nucleic acids: structures, properties and functions. University Science Book, Sausalito

Bradley DA, Hugtenburg RP, Yusoff AL (2006a) Near-edge elastic photon scattering from dilute aqueous ions. Radiat Phys Chem 75:2129–2135. doi:10.1016/j.radphyschem.2005.12.033

Bradley DA, Hugtenburg RP, Yusoff AL (2006b) At-edge minima in elastic photon scattering amplitudes for dilute aqueous ions. Radiat Phys Chem 75:1676–1682. doi:10.1016/j.radphyschem.2005.11.029

Bram S, Butler-Browne G, Baudy P, Ibel K (1975) Quaternary structure of chromatin. Proc Natl Acad Sci U S A 72:1043–1045. doi:10.1073/pnas.72.3.1043

Buning R, Van Noort J (2010) Single-pair FRET experiments on nucleosome conformational dynamics. Biochimie 92:1729–1740. doi:10.1016/j.biochi.2010.08.010

Chang SL, Chen SH, Rill RL, Lin JS (1990) Measurements of monovalent and divalent counterion distributions around persistence length DNA fragments in solution. J Phys Chem 94:8025–8028. doi:10.1021/J100384a010

Chaudhuri BN (2015) Emerging applications of small angle solution scattering in structural biology. Protein Sci 24:267–276. doi:10.1002/pro.2624

Chen Y, Tokuda JM, Topping T et al (2014) Revealing transient structures of nucleosomes as DNA unwinds. Nucleic Acids Res 42:8767–8776. doi:10.1093/nar/gku562

Chin K, Sharp KA, Honig B, Pyle AM (1999) Calculating the electrostatic properties of RNA provides new insights into molecular interactions and function. Nat Struct Biol 6:1055–1061

Chu VB, Bai Y, Lipfert J et al (2007) Evaluation of ion binding to DNA duplexes using a size-modified Poisson-Boltzmann theory. Biophys J 93:3202–3209. doi:10.1529/biophysj.106.099168

Clark DJ, Kimura T (1990) Electrostatic mechanism of chromatin folding. J Mol Biol 211:883–896. doi:10.1016/0022-2836(90)90081-V

Curry S (2015) Structural biology: a century-long journey into an unseen world. Interdiscip Sci Rev 40:1–10. doi:10.1179/0308018815Z.000000000120

Das R, Mills TT, Kwok LW et al (2003) Counterion distribution around DNA probed by solution x-ray scattering. Phys Rev Lett 90:188103

Draper DE (2004) A guide to ions and RNA structure. RNA 10:335–343. doi:10.1261/rna.5205404.and

Gansen A, Tóth K, Schwarz N, Langowski J (2009a) Structural variability of nucleosomes detected by single-pair Förster resonance energy transfer: Histone acetylation, sequence variation, and salt effects. J Phys Chem B 113:2604–2613. doi:10.1021/jp7114737

Gansen A, Valeri A, Hauger F et al (2009b) Nucleosome disassembly intermediates characterized by single-molecule FRET. Proc Natl Acad Sci U S A 106:15308–15313. doi:10.1073/pnas.0903005106

Gansen A, Toth K, Schwarz N, Langowski J (2015) Opposing roles of H3- and H4-acetylation in the regulation of nucleosome structure–a FRET study. Nucleic Acids Res 43:1433–1443. doi:10.1093/nar/gku1354

Giambaşu GM, Luchko T, Herschlag D et al (2014) Ion counting from explicit-solvent simulations and 3D-RISM. Biophys J 106:883–894. doi:10.1016/j.bpj.2014.01.021

Glatter O, Kratky O (1982) Small angle x-ray scattering. Academic, London

Gopal A, Zhou ZH, Knobler CM, Gelbart WM (2012) Visualizing large RNA molecules in solution. RNA 18:284–299. doi:10.1261/rna.027557.111

Graewert MA, Svergun DI (2013) Impact and progress in small and wide angle x-ray scattering (SAXS and WAXS). Curr Opin Struct Biol 23:748–754. doi:10.1016/j.sbi.2013.06.007

Grochowski P, Trylska J (2007) Continuum molecular electrostatics, salt effects, and counterion binding–a review of the Poisson-Boltzmann Theory and its modifications. Biopolymers 89:93–113. doi:10.1002/bip

Guinier A, Fournet G (1955) Small-angle scattering of x-rays. Wiley, New York

Hagerman P (1988) Flexibility of DNA. Annu Rev Biophys Biomol Struct 17:265–286. doi:10.1146/annurev.biophys.17.1.265

Hansen JC (2002) Conformational dynamics of the chromatin fiber in solution: determinants, mechanisms, and functions. Annu Rev Biophys Biomol Struct 31:361–392. doi:10.1146/annurev.biophys.31.101101.140858

Hernan GG, Grayson P, Lin H et al (2007) Biological consequences of tightly bent DNA: the other life biological of a macromolecular celebrity. Biopolymers 85:115–130. doi:10.1002/bip.20627. Biological

Hjelm RP, Kneale GG, Suau P et al (1977) Small angle neutron scattering studies of chromatin subunits in solution. Cell 10:139–151. doi:10.1016/0092-8674(77)90148-9

Hoch DA, Stratton JJ, Gloss LM (2007) Protein-protein förster resonance energy transfer analysis of nucleosome core particles containing H2A and H2A.Z. J Mol Biol 371:971–988. doi:10.1016/j.jmb.2007.05.075

Holst M, Baker N, Wang F (2000) Adaptive multilevel finite element solution of the Poisson-Boltzmann equation I. Algorithms and examples. J Comput Chem 21:1319–1342. doi:10.1002/1096-987X(20001130)21:15<1319::AID-JCC1>3.0.CO;2-8

Ibel K, Stuhrmann HB (1975) Comparison of neutron and x-ray scattering of dilute myoglobin solutions. J Mol Biol 93:255–265. doi:10.1016/0022-2836(75)90131-X

Inoko Y, Yamamoto M, Satoru F, Ueki T (1992) X-ray scattering study of the shape of the DNA region core particle with synchrotron radiation in nucleosome Yoji Inoko', Masaki Yamamoto, 2 Satoru Fujiwara, and Tatzuo Ueki2 of Biophysical Engineering, Faculty of Engineering Science, Osaka Received. Structure 316:310–316

Jacques DA, Trewhella J (2010) Small-angle scattering for structural biology-expanding the frontier while avoiding the pitfalls. Protein Sci 19:642–657. doi:10.1002/pro.351

Kazantsev AV, Rambo RP, Karimpour S et al (2011) Solution structure of RNase P RNA. RNA 17:1159–1171. doi:10.1261/rna.2563511

Koch MH, Vachette P, Svergun DI (2003) Small-angle scattering: a view on the properties, structures and structural changes of biological macromolecules in solution. Q Rev Biophys 36:147–227

Kornberg RD, Lorch Y (1999) Twenty-five years of the nucleosome, fundmamental particle of the eukaryotic chromosome. Cell 98:285–294

Korolev N, Vorontsova OV, Nordenskiöld L (2007) Physicochemical analysis of electrostatic foundation for DNA-protein interactions in chromatin transformations. Prog Biophys Mol Biol 95:23–49. doi:10.1016/j.pbiomolbio.2006.11.003

Korolev N, Allahverdi A, Yang Y et al (2010) Electrostatic origin of salt-induced nucleosome array compaction. Biophys J 99:1896–1905. doi:10.1016/j.bpj.2010.07.017

Li M, Wang MD (2012) Unzipping single DNA molecules to study nucleosome structure and dynamics. In: Wu C, Allis CD (eds) Methods in Enzymology, vol. 513. Academic, Burlington, pp. 29-58

Li G, Widom J (2004) Nucleosomes facilitate their own invasion. Nat Struct Mol Biol 11:763–769. doi:10.1038/nsmb801

Lipfert J, Doniach S (2007) Small-angle x-ray scattering from RNA, proteins, and protein complexes. Annu Rev Biophys Biomol Struct 36:307–327. doi:10.1146/annurev.biophys.36.040306.132655

Lipfert J, Doniach S, Das R, Herschlag D (2014) Understanding nucleic acid-ion interactions. Annu Rev Biochem 83:813–841. doi:10.1146/annurev-biochem-060409-092720

Liu HB, Shi YM, Chen XS, Warshel A (2009) Simulating the electrostatic guidance of the vectorial translocations in hexameric helicases and translocases. Proc Natl Acad Sci U S A 106:7449–7454. doi:10.1073/pnas.0900532106

Lohman TM, Overman LB (1985) 2 Binding modes in escherichia-coli single-strand binding protein-single stranded DNA complexes - modulation by nacl concentration. J Biol Chem 260:3594–3603

Luger K, Phillips SE (2010) Rise of the molecular machines. Curr Opin Struct Biol 20:70–72. doi:10.1016/j.sbi.2010.01.006

Luger K, Mäder AW, Richmond RK et al (1997) Crystal structure of the nucleosome core particle at 2.8 A resolution. Nature 389:251–260. doi:10.1038/38444

Luscombe NM, Austin SE, Berman HM, Thornton JM (2000) An overview of the structures of protein-DNA complexes. Genome Biol:11–37

Luzzati V, Masson F, Mathis A (1967) X-ray scattering study of rigid polyelectrolyte solution. lithium, sodium, and cesium salts of DNA. Biopolymers 5:491–508

Manning GS (1969) Limiting laws and counterion condensation in polyelectrolyte solutions I. Colligative Properties. J Chem Phys 51:924. doi:10.1063/1.1672157

Marko JF, Siggia ED (1995) Stretching DNA. Macromolecules 28:8759–8770. doi:10.1021/ma00130a008

Martin E, Saenger W (2013) Principles of nucleic acid structure. Springer, New York

Meisburger SP, Pabit SA, Pollack L (2015) Determining the locations of ions and water around DNA from X-ray scattering measurements. Biophys J 108:2886–2895. doi:10.1016/j.bpj.2015.05.006

Mihardja S, Spakowitz AJ, Zhang Y, Bustamante C (2006) Effect of force on mononucleosomal dynamics. Proc Natl Acad Sci U S A 103:15871–15876. doi:10.1073/pnas.0607526103

Morfin I, Horkay F, Basser PJ et al (2004) Adsorption of divalent cations on DNA. Biophys J 87:2897–2904. doi:10.1529/biophysj.104.045542

Mouat MF, Manchester KL (1998) The intracellular ionic strength of red cells and the influence of complex formation. Comp Haematol Int 8:58–60

Ngo TTM, Ha T (2015) Nucleosomes undergo slow spontaneous gaping. Nucleic Acids Res 43:1–8. doi:10.1093/nar/gkv276

Ngo TTM, Zhang Q, Zhou R et al (2015) asymmetric unwrapping of nucleosomes under tension directed by DNA Local Flexibility. Cell 160:1135–1144. doi:10.1016/j.cell.2015.02.001

Nguyen HT, Pabit SA, Meisburger SP et al (2014) Accurate small and wide angle x-ray scattering profiles from atomic models of proteins and nucleic acids. J Chem Phys 141:22D508. doi:10.1063/1.4896220

Orthaber D, Bergmann A, Glatter O (2000) SAXS experiments on absolute scale with Kratky systems using water as a secondary standard. J Appl Crystallogr 33:218–225. doi:10.1107/S0021889899015216

Pabit SA, Finkelstein KD, Pollack L (2009) Using anomalous small angle X-ray scattering to probe the ion atmosphere around nucleic acids. Methods Enzymol 37:3887–3896

Pabit SA, Qiu X, Lamb JS et al (2009b) Both helix topology and counterion distribution contribute to the more effective charge screening in dsRNA compared with dsDNA. Nucleic Acids Res 37:3887–3896. doi:10.1093/nar/gkp257

Pabit SA, Meisburger SP, Li L et al (2010) Counting ions around DNA with anomalous small-angle x-ray scattering. J Am Chem Soc 132:16334–16336. doi:10.1021/ja107259y

Pardon JF, Worcester DL, Wooley JC et al (1975) Low-angle neutron scattering from chromatin subunit particles. J Chem Inf Model 2:2163–2176. doi:10.1017/CBO9781107415324.004

Park S, Bardhan JP, Roux B, Makowski L (2009) Simulated x-ray scattering of protein solutions using explicit-solvent models. J Chem Phys 130:1–8. doi:10.1063/1.3099611

Pérez J, Nishino Y (2012) Advances in x-ray scattering: from solution SAXS to achievements with coherent beams. Curr Opin Struct Biol 22:670–678. doi:10.1016/j.sbi.2012.07.014

Pollack L (2011) SAXS studies of ion-nucleic acid interactions. Annu Rev Biophys 40:225–242. doi:10.1146/annurev-biophys-042910-155349

Prinsen P, Schiessel H (2010) Nucleosome stability and accessibility of its DNA to proteins. Biochimie 92:1722–1728. doi:10.1016/j.biochi.2010.08.008

Richmond TJ, Davey CA (2003) The structure of DNA in the nucleosome core. Nature 423:145–150. doi:10.1038/nature01595

Rocchia W, Alexov E, Honig B (2001) Extending the applicability of the nonlinear Poisson-Boltzmann equation: multiple dielectric constants

and multivalent ions. J Phys Chem B 105:6507–6514. doi:10.1021/jp010454y

Rohs R, Jin X, West SM et al (2010) Origins of specificity in protein-DNA recognition. Annu Rev Biochem 79:233–269. doi:10.1146/annurev-biochem-060408-091030

Sardet C, Tardieu A, Luzzati V (1976) Shape and size of bovine rhodopsin: a small-angle x-ray scattering study of a rhodopsin-detergent complex. J Mol Biol 105:383–407. doi:10.1016/0022-2836(76)90100-5

Shlyakhtenko LS, Lushnikov AY, Lyubchenko YL (2009) Dynamics of nucleosomes revealed by time-lapse atomic force microscopy. Biochemistry 48:7842–7848. doi:10.1021/bi900977t

Skou S, Gillilan RE, Ando N (2014) Synchrotron-based small-angle x-ray scattering of proteins in solution. Nat Protoc 9:1727–1739. doi:10.1038/nprot.2014.116

Stoddard CD, Montange RK, Hennelly SP et al (2010) Free state conformational sampling of the SAM-I riboswitch aptamer domain. Structure 18:787–797. doi:10.1016/j.str.2010.04.006.Free

Stuhrmann HB (1974) Neutron small-angle scattering of biological macromolecules in solution. J Appl Crystallogr 7:173–178. doi:10.1107/S0021889874009071

Stuhrmann HB, Kirste RG (1965) Elimination Der Intrapartikularen Untergrundstreuung Bei Der Rontgenkleinwinkelstreuung an Kompakten Teilchen (Proteinen). Z Phys Chem-Frankfurt 46:247

Stuhrmann HB, Miller A (1978) Small-angle scattering of biological structures. J Appl Crystallogr 11:325–345. doi:10.1107/S0021889878013473

Svergun DI (1992) Determination of the regularization parameter in indirect-transform methods using perceptual criteria. J Appl Crystallogr 25:495–503. doi:10.1107/S0021889892001663

Svergun DI, Koch MHJ (1994) Structural model of the 50 S subunit of escherichia coli ribosomes from solution scattering. J Mol Biol 240:66–77

Svergun DI, Koch MHJ (2003) Small-angle scattering studies of biological macromolecules in solution. Rep Prog Phys 66:1735–1782. doi:10.1088/0034-4885/66/10/R05

Svergun DI, Pedersen JS, Serdyuk IN, Koch MHJ (1994) Solution scattering from 50S ribosomal subunit resolves inconsistency between electron microscopic models. Proc Natl Acad Sci U S A 91:11826–11830

Svergun DI, Koch MHJ, Timmins PA, May RP (2013) Small angle x-ray and neutron scattering from solutions of biological macromolecules. Oxford University Press, Oxford

Sztucki M, Di Cola E, Narayanan T (2012) Anomalous small-angle x-ray scattering from charged soft matter. Eur Phys J Spec Top 208:319–331. doi:10.1140/epjst/e2012-01627-x

Tang C, Loeliger E, Luncsford P et al (2004) Entropic switch regulates myristate exposure in the HIV-1 matrix protein. Proc Natl Acad Sci U S A 101:517–522. doi:10.1073/pnas.0305665101

Tardieu A, Mateu L, Sardet C et al (1976) Structure of human serum lipoproteins in solution. II. Small-angle x-ray scattering study of HDL3 and LDL. J Mol Biol 101:129–153. doi:10.1016/0022-2836(76)90368-5

Thommes P, Hubscher U (1992) Review: eukaryotic DNA helicases: essential enzymes for DNA transactions. Chromosoma 101:467–473. doi:10.1007/BF00352468

Tims HS, Gurunathan K, Levitus M, Widom J (2011) Dynamics of nucleosome invasion by DNA binding proteins. J Mol Biol 411:430–448. doi:10.1016/j.jmb.2011.05.044

Ueki T, Inoko Y, Kataoka M et al (1986) X-ray scattering study on hemoglobin solution with synchrotron radiation: a simple analysis of scattering profile at moderate angles in terms of arrangement of subunits. J Biochem 99:1127–1136

Vestergaard B, Sayers Z (2014) Investigating increasingly complex macromolecular systems with small-angle x-ray scattering. IUCrJ 1:523–529. doi:10.1107/S2052252514020843

Vlijm R, Lee M, Lipfert J et al (2015) Nucleosome assembly dynamics involve spontaneous fluctuations in the handedness of tetrasomes. Cell Rep 10:216–225. doi:10.1016/j.celrep.2014.12.022

Widom J (1998) Structure, dynamics, and function of chromatin in vitro. Annu Rev Biophys Biomol Struct 27:285–327. doi:10.1146/Annurev.Biophys.27.1.285

Wong GCL, Pollack L (2010) Electrostatics of strongly charged biological polymers: ion-mediated interactions and self-organization in nucleic acids and proteins. Annu Rev Phys Chem 61:171–189. doi:10.1146/annurev.physchem.58.032806.104436

Yager TD, McMurray CT, van Holde KE (1989) Salt-induced release of DNA from nucleosome core particles. Biochemistry 28:2271–2281. doi:10.1021/bi00431a045

You H, Iino R, Watanabe R, Noji H (2012) Winding single-molecule double-stranded DNA on a nanometer-sized reel. Nucleic Acids Res 1–6. doi: 10.1093/nar/gks651

Zlatanova J, Bishop TC, Victor JM et al (2009) The nucleosome family: dynamic and growing. Structure 17:160–171. doi:10.1016/j.str.2008.12.016

Zuo X, Cui G, Merz KM et al (2006) X-ray diffraction "fingerprinting" of DNA structure in solution for quantitative evaluation of molecular dynamics simulation. Proc Natl Acad Sci U S A 103:3534–3539. doi:10.1073/pnas.0600022103